Design and Optimization of a Disaggregated Constellation for Space Situational Awareness

Adam Snow*, Angela den Boer†, Luke Alexander‡
Georgia Institute of Technology, Atlanta, GA 30332-0150, USA

Advisor: Marcus J. Holzinger§
Georgia Institute of Technology, Atlanta, GA 30332-0150, USA

Abstract

The number of objects in earth orbit is increasing at an unprecedented rate, increasing the need for space situational awareness. A novel approach for the design and optimization of a disaggregated and scalable satellite constellation for space object detection is proposed. Discussions of the payload design objectives and detection constraints are presented with respect to the design process. To understand the effect of detection capabilities for a space based sensor, a series of simulations were performed using the publicly available JSpOC catalog through varying constellation architectures. A genetic algorithm was employed to explore the objective space of constellation architectures in order to optimize mission performance. In particular, this optimization effort seeks to maximize economic return of the space mission by quantifying the financial value of mission performance.

I. Introduction

Growth of the space industry has given the area in which spacecraft operate an intrinsic value in and of itself. Although largely theoretical when it was proposed, the "Kessler Syndrome", a cascading of collisions between orbiting objects rendering Earth orbit inaccessible for generations [1], is a concerning possibility in the near future. Decades of "big sky" mentality regarding Space Objects (SOs) have left a Low Earth Orbit (LEO) environment that is growing more and more crowded with debris: functional satellites, non-functional satellites, rocket bodies, and everything else placed into orbit that has not yet come down. The majority of information about SOs comes from the U.S. Space Surveillance Network (SSN), a network of ground- and space-based assets dedicated to tracking satellites, space debris, and all objects in Earth orbit [2]. Data from the SSN is reported to and subsequently made publicly available by the Department of Defense's Joint Space Operations Command (JSpOC) [3]. JSpOC currently places the number of objects in LEO larger than 10 cm at more than 21,000.

Given that the majority of SSN sensors are ground-based radar arrays, only objects that are larger than 10 cm in diameter can be consistently tracked. Rayleigh scattering makes smaller objects difficult to consistently detect [4] and therefore objects smaller than 10 cm cannot be cataloged. As such, the recorded numbers of objects below 10 cm are only estimates: approximately 500,000 SOs between 1 cm and 10 cm in diameter [5] and many millions of SOs below 1 cm in diameter [6]. The situation is difficult to characterize even as it continues to worsen. Events such as the 2007 Chinese Anti-Satellite Fengyun-3 test [7] and the 2009 collision between the defunct Cosmos-2251 satellite and the operational Iridium-33 satellite have both significantly worsened the situation. These two events alone doubled the number of SOs larger than 1 cm, producing over 250,000 new pieces of space debris [8]. Despite international criticism, it is suspected

*Masters Student, School of Aerospace Engineering; Email: asnow6@gatech.edu
†Masters Student, School of Aerospace Engineering; Email: adenboer3@gatech.edu
‡Undergraduate Student, School of Aerospace Engineering; Email: lukealexander@gatech.edu
§Assistant Professor, School of Aerospace Engineering, AIAA Senior Member, Email: holzinger@gatech.edu

that on-orbit ASAT tests such as those in 2013 and 2014 [9] will continue. JSpOC catalogs reveal that only 7% of SOs are operational assets. This leaves 93% of the objects in orbit uncontrollable [11]. The severity of the issue becomes apparent when considering its impact on operational missions; orbital debris larger than 10 cm can cause catastrophic failure in most space missions, and debris between 1 and 10 cm can easily disable or damage core mission functionality [10].

Such a dire situation has caused concerns over the long term health of the space environment. The United States has identified Space Situational Awareness (SSA) as one of the most important goals of space technology development over the coming years. The Presidential Space Policy calls for increased knowledge of our space environment [12]. Publication 3-14 from the Joint Chiefs of Staff calls for increased SSA as one of the most important areas of technology development for the coming decade [13, 14]. Indeed, some of the most recent Congressional budgets include requests from the US Air Force for up to $6.5 billion for increased SSA as well [15] in hopes that innovative solutions will protect the space environment for years to come. In terms of global resolution, the United Nations Committee on the Peaceful Uses of Outer Space has also urged international cooperation on SSA as an issue that affects all space-faring nations equally [16].

While many attempts have been made to accurately characterize the current situation of debris in earth orbit, few attempts have been made to do so in a disaggregated manner. The SBSS mission is a planned constellation of satellites for on-orbit SSA, but has yet to be fully deployed. Likewise, Space Fence consists of two ground-based radar arrays, but is not planned to scale any further [17]. A design paradigm that has yet to be implemented to address the SSA problem is a constellation of small satellites. The design objectives of such a constellation are delineated to allow the requirements of the mission to drive the capabilities of the satellite. Various sensor sizing metrics are described to demonstrate that a small satellite constellation can be feasibly created. The standard detection constraints for all space based optical systems – line of sight, illumination, and visual magnitude – are detailed in their relevance to the simulation and of system capabilities. Once the parameters of the system have been defined, a detailed simulation of mission performance will be performed. Finally, an genetic algorithm is employed to optimize the economic return of the proposed satellite constellation.

II. Design Objectives and Sensor Sizing

SSA mission architectures dictate a need to detect as many objects as possible, detect the dimmest objects possible, and obtain detections with as much accuracy as possible, providing criteria by which the system's optical sensor can be sized. While many parameters affect the performance of an optical sensor, aperture diameter D, pixel size p, and f-number N can be used to more easily quantify the performance of a given optical system, assuming all other parameters relevant to sensor sizing are assigned constant values [21]. An analysis on these three sizing parameters can narrow prospective optics choices, but is not considered a means to obtain a final system design.

By leveraging the three parameters stated above, the instantaneous field of view or IFOV for a given optical system can be defined.

$$IFOV = 2tan^{-1}\left(\frac{p}{2ND}\right) \tag{1}$$

IFOV can be described as the field of view for a single pixel. This parameter is important in determining the overall field of view or FOV for an optical sensor, as well as affecting the accuracy of a system. The following equation shows how to calculate the vertical and horizontal components of FOV, FOV_v and FOV_h respectively, where n_p is the number of pixels in a given sensor in each direction.

$$FOV_v = n_{p,v} IFOV \tag{2}$$

$$FOV_h = n_{p,h} IFOV \tag{3}$$

Optical systems with larger FOVs are capable of detecting a higher volume of objects per frame; however, because a sensor with a larger IFOV captures photons from a larger area, the

precise location of any detected object will be less accurately defined. A tradeoff must be made between increased detection and accuracy of detection with regard to IFOV. This trade informs all three design parameters, D, N, and p. The impact of this tradeoff can be mitigated by choosing a sensor with a larger pixel count, but consideration must be given to other aspects of sensor design such as power draw and physical dimensions. Additionally, a higher FOV sensor will be capable of detecting objects with higher angular velocities, given shorter integration times [22], which can simplify processing of frames.

To quantify the limiting magnitude, or dimmest magnitude observable by an optical system, a metric for magnitude needs to be defined. In Equations 4 through 6, m_v is the limiting magnitude. The equation has been split into smaller equations here in the interest of space.

$$h_1 = SNR_{alg}[\sqrt{m_i}\omega ND(q_{sky} + q_{dark})]^{1/2} \quad (4)$$

$$h_2 = \Phi_0 \tau_{atm} \tau_{opt} \left(\frac{\pi D^2}{4}\right) QE\sqrt{p} \quad (5)$$

$$m_v = -2.5 log_{10}\left[\frac{h_1}{h_2}\right] \quad (6)$$

The above equation, developed by Coder and Holzinger [21], incorporates a minimum detectable signal to noise ratio, or SNR, which is defined as the ratio of photons emitted by the target object to the photons emitted by all other noise sources. m_i is the number of pixel occupied by an SO, ω is the relative velocity between the sensor and the SO, q_{sky} is background radiance intensity per pixel, q_{dark} is dark current per pixel, Φ_0 is the spectral excitance of a magnitude 0 object, τ_{atm} is atmospheric transmittance, τ_{opt} is optical transmittance, and QE is the quantum efficiency of a given sensor . Again, a higher limiting magnitude indicates that dimmer objects can be detected, so it is desirable to maximize this value. In terms of design parameters, this implies higher f-number, N, and lower aperture diameter, D.

Features can be extracted from an image using any number of open source codes for feature or blob detection. Feature centroids are extracted from an image based on an intensity threshold. This threshold can be dynamically calculated for each frame in order to more accurately detect as many features as possible while limiting false detections due to noise or other image imperfections such as Earthshine.

Once an optical system has been selected for a mission, high level algorithms for processing images extracted from the sensor. Differentiating between stars and SOs can be expressed as a comparison of relative velocities of detected features [23]. The assumption must be made that more than half of the features detected in a given image are stars. Stars will move in a similar fashion, while SOs will deviate from this average. Then, by calculating a rotation and translation of frames necessary to align the greatest number of features, stars can be identified and removed from the frames. Remaining features can then be classified as SOs. Due to intermittent detection of some objects on the edge of the sensor's limiting magnitude for a given expose time, there is the potential for some misclassified objects. If, however, objects are tracked from frame to frame, tracks of objects that have non-uniform detection history can be maintained from further frames.

Features that have been identified as stars can be matched to star catalog IDs by using a Lost in Space or LIS algorithm [20]. This method assumes no previous knowledge of pointing attitude and matches stars based on angular distances. Once stars have been associated with inertial bearings given in a star catalog, these values can be used to calculate inertial bearings of any SOs in the same frame. This process is repeated for each frame and a list of objects can be compiled for a set of images taken with the optical payload. The resulting data product can be a list of inertial bearings, or right ascensions and declinations, for each SO.

III. Detection Constraints

Before carrying out an analysis of the detectability of objects, it is convenient to establish a constant coordinate system in which one can work. This analysis, as with others [24], is carried out with the I, J, and K positions

and velocities of the objects and the observer being fixed in the Earth Centered Inertial (ECI) frame. The position of the observer is denoted as $\mathbf{o}$ and the position of the SO can be denoted as $\mathbf{r}$. The distance between these two vectors is defined as the line of sight (LOS) from the observer to the objects, $\mathbf{v}$. The center of the FOV of the optic is defined as $\hat{\mathbf{p}}$. The sun vector is defined as the unit vector in the direction from the object to the sun, $\hat{\mathbf{s}}$. Calculation of reflectivity requires the angle between the LOS and the sun, and so ψ, the solar phase angle, is also defined. With the radius of the earth being $\mathbf{R}_e$, the LOS would be tangent to the surface of the earth when $\mathbf{v}$ is equal to $\mathbf{v}_{||}$ at an angle θ from the observer. All of this notation can be visualized in Figure 1.

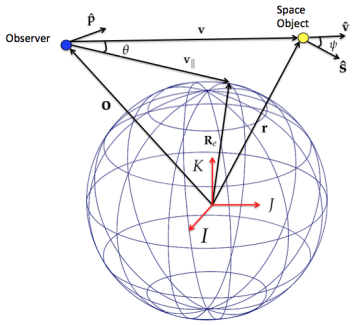

Figure 1: *The relationship between an observer and an SO in orbit around Earth.*

III.1. Line Of Sight

At this point, LOS equations can be derived to define which objects are geometrically possible for an observer to see. The angle θ between $\mathbf{v}_{||}$ and $\mathbf{v}$ is used to define angles at which the Earth will not be between an object and the observer. The Earth radius at the tangent point is denoted as R_e such that inspection will yield that $\|\mathbf{R}_e\|^2 + \|\mathbf{v}_{||}\|^2 = \|\mathbf{o}\|^2$. Continuing this analysis, the following equations can define LOS condition for a given SO:

$$cos\theta = \frac{\sqrt{\|\mathbf{o}\|^2 - \|\mathbf{R}_e\|^2}}{\|\mathbf{o}\|} \tag{7}$$

$$\mathbf{o} \cdot \mathbf{v} \geq -cos(\theta)\|\mathbf{o}\|\|\mathbf{v}\| \tag{8}$$

The inequality shown in Equation 9 can then be derived via the substitution of Equation 7 into Equation 8. Equation 9 will be true if the SO is in the LOS of the observer, and will be false if the SO is not in the LOS of the observer.

$$\mathbf{o} \cdot \hat{\mathbf{v}} + \sqrt{\|\mathbf{o}\|^2 - \|\mathbf{R}_e\|^2} \geq 0 \tag{9}$$

III.2. Illumination

Objects that are located in the earth's shadow will not be illuminated by the sun and will therefore not be visible to the observer. For the sun vector $\hat{\mathbf{s}}$ defined in Figure 1, the following two conditions must be satisfied for an object to be eclipsed by the Earth:

$$\mathbf{r} \cdot \hat{\mathbf{s}} > 0 \tag{10}$$

$$\|\hat{\mathbf{s}} \times \mathbf{r}\| \leq R_e \tag{11}$$

III.3. Signal to Noise Ratio

While the limiting and visual magnitude of an object are both useful for abstract determination of optical payload performance, they are not ideal metrics for defining detectability of an object. Instead, relations involving the visual magnitude of objects can be used to derive the signal to noise ratio (SNR) of an object. The SNR can be much more useful for simulation as it can be manipulated to serve as a function of distance between the observer and the object, $\|\mathbf{v}\|$, and parameters of the payload and environment.

In deriving an applicable form of this equation, one must first define ψ using the coordinate system outlined in Figure 1. The total reflectivity, a, of an object is defined as the sum of the specular and diffuse components of reflectivity as functions of ψ.

$$\psi = \arccos\left(\frac{\mathbf{v} \cdot \mathbf{s}}{\|\mathbf{v}\| \cdot \|\mathbf{s}\|}\right) \tag{12}$$

$$a = a_{diff}(\psi) + a_{spec}(\psi) \tag{13}$$

Having defined the reflectivity, an equation for visual magnitude can be developed. The radius of the object r defines the area $A = 2\pi r$. The distance to the object, $\rho = \|\mathbf{v}\|$, and the reflectivity of an object, a, respectively, are then parameters of an equation for the conservative

approximation for the visual magnitude of a spherical object in the vacuum of space [24].

$$m_{SO} = m_{sun} - 2.5log\left(\frac{A\alpha a}{\rho^2}\right) \tag{14}$$

In Equation 14, the illuminated area of an SO is A, and the albedo of the SO is $\alpha \in [0, 1]$. The following substitution will be made in further calculations.

$$b = A\alpha a \tag{15}$$

The mean value for the albedo of space debris has recently been estimated as 0.175 [25]. This value will be used for both α and a_{spec} in simulation. a_{diff} can be calculated from the geometry of the two objects as defined in [21]. SNR is defined as the ratio between the average number of photons from an SO and the standard deviation of photon flux from all noise sources [21]. SNR is defined below in Equation 16 with substitutions made for simplicity.

$$SNR = \frac{q_{SO}t}{\sqrt{q_{SO}t + c}} \tag{16}$$

$$c = m\left(1 + \frac{1}{z}\right)\left[(q_{sky} + q_{dark})t + \frac{\sigma_r^2}{n^2}\right] \tag{17}$$

The average number of photons from the SO can be approximated as the photon flux q_{SO} multiplied by integration time t with the standard deviation of photon flux from all noise sources is the square root of the average number of photons from the SO plus c. c is defined as the sum of all other noise sources: $q_{p,sky}$ and $q_{p,dark}$ as defined earlier, m being number of pixels occupied by an SO, z being the number of pixels without an SO, σ_r^2 being the read noise of the camera, and n being pixel binning factor. It is important to note that q_{SO} is the only term in the above SNR equation that varies with distance from observer to SO ρ. As such, the minimum photon flux necessary to detect an object q_{min} can be written as a quadratic in terms of the minimum SNR SNR_{min} and integration time t.

$$q_{SO}^2\left(\frac{t_{int}}{SNR_{min}}\right)^2 - q_{SO}t_{int} - c = 0 \tag{18}$$

$$q_{min} = \frac{SNR_{min}^2}{2t_{int}^2}\left(t_{int} + \sqrt{t_{int}^2 + 4\frac{t_{int}^2}{SNR_{min}^2}c}\right) \tag{19}$$

Only the positive, real root of q_{SO} is considered as a negative or imaginary root would only be valid for a photon source, rather than a photon detector. Another form of q_{SO} can also be determined from the total spectral excitance of the SO Φ_{SO}, the transmittance of the atmosphere and the optic $\tau_{atm}, \tau_{opt} \in [0, 1]$, the quantum efficiency of the camera QE, and the diameter of the lens D [21].

$$q_{SO} = \Phi_{SO}\tau_{atm}\tau_{opt}\left(\frac{\pi D^2}{4}\right)QE \tag{20}$$

Given the definition for Φ_{SO} for a constant Φ_0 for a magnitude zero object [21],

$$\Phi_{SO} = \Phi_0 \times 10^{-.4m_{SO}} \tag{21}$$

This equation can be simplified, as space based optical sensors need not take the transmittance of the atmosphere into account, i.e. $\tau_{atm} = 1$.

$$q_{SO} = \Phi_{SO}\tau_{opt}\left(\frac{\pi D^2}{4}\right)QE \tag{22}$$

Defining q_{opt} as

$$q_{opt} = \tau_{opt}\left(\frac{\pi D^2}{4}\right)QE\Phi_0 \tag{23}$$

$$q_{SO} = q_{opt} \times 10^{-.4m_{SO}} \tag{24}$$

Substituting q_{min} as q_{SO}

$$m_{SO} = -2.5log_{10}\left(\frac{q_{min}}{q_{opt}}\right) \tag{25}$$

Substituting Equation 25 into Equation 14 and making the appropriate substitutions yields:

$$2.5log_{10}\left(\frac{q_{min}}{q_{opt}}\right) + m_{sun} = 2.5log_{10}\left(\frac{b}{\rho^2}\right) \tag{26}$$

Defining m_{req} as

$$m_{req} = 2.5log_{10}\left(\frac{q_{min}}{q_{opt}}\right) + m_{sun} \tag{27}$$

A final form of maximum range ρ_{max} as a function of SNR_{min} and t can now be obtained:

$$\rho \leq \rho_{max} = \sqrt{\frac{b}{10^{.4m_{req}}}} \tag{28}$$

The three constraints on object detection: line of sight, illumination, and signal to noise ratio are now defined. The reader will note that these three constraints vary solely on the geometry of the coordinate system in Figure 1 and the performance of the optical payload. As such, assumptions may be made about the optical payload to simulate the performace of an observation platform through a variety of orbital parameters.

Using the following values for nominal small satellite payload parameters , a plot of ρ vs. SNR can be obtained.

Table 1: *Nominal small satellite optical payload parameters for calculation of ρ vs SNR_{min}*

Variable	Value	Units
ψ	$\frac{\pi}{3}$	radians
t	.1	seconds
Φ_0	5.636×10^{10}	photons/s/m^2
D	.075	meters
N	.8	N/A
f	N*D	meters
QE	.6	N/A
z	1024*1280*.1	pixels
m	5	pixels
$q_{p,dark}$	.5	photons/s/pixel
$q_{p,sky}$	.5	photons/s/pixel
τ_{opt}	.9	N/A
σ_r^2	9	photons/s/pixel
n	1	N/A
SNR_{min}	4	N/A

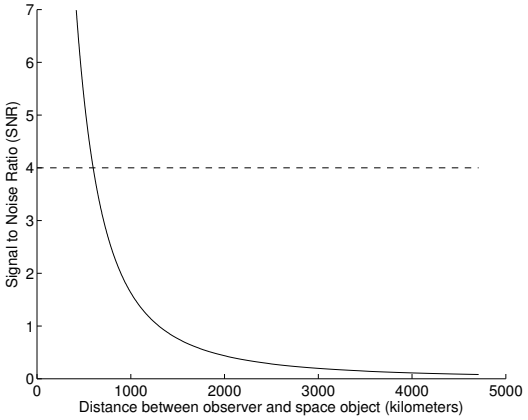

Figure 2: *The range at which an observer can detect an object as a function of SNR. A nominal SNR value of 4 would yield detectability of an object 1 cm in diameter at approximately 600 km.*

IV. Constellation Design

The performance of many space missions is enhanced through the utilization of a constellation architecture. For space situational awareness missions, constellations are particularly valuable for maximizing the quantity of detections from a space based platform. By deploying multiple sensors that are distributed throughout the orbit environment, a constellation based SSA mission can significantly increase detection performance. The recent developments in small satellite systems have given rise to several other benefits in constellation design as well [31]. First, a constellation architecture is by definition a fractionated and disaggregated system that is resilient to fault. By utilizing a series of identical satellites, a constellation is more resilient to individual satellite failure. Second, constellations are highly scalable in that they can be incrementally deployed. This provides financial and operational flexibility for mission planners, not requiring the entire system to be deployed in a single launch. Finally, this incremental deployment results in a much higher technology refreshment rate than larger satellite missions. With a shorter life time and scalable architecture, sequential satellite deployments can take advantage of incremental technology improvements, leading to more adaptive system architectures. These

benefits make the utilization of a constellation architecture highly attractive in the design of a space situational awareness campaign.

IV.1. Performance Simulation

A thorough discussion of the parameters describing payload design and detection capability has been presented. To quantify the effects of these parameters on a space mission, a detailed space situational awareness mission simulator has been developed. This simulator leverages much of the work done at Georgia Tech in the realm of space situational awareness and propagation modeling [24].

The simulation begins by generating a fixed set of surveillance spacecraft that are placed in a low earth orbit. These simulated satellites employ the same payload parameters presented in Table 1 and are representative of the capabilities typical of small satellites. These spacecraft are propagated over a given sample period and are aligned with their sensors directed along the prograde vector. Fixed step two-body propagation is deemed sufficiently accurate for short simulations and the application at hand.

Next, the 15,106 known SOs contained in the 2015 Space Object Catalog (SOC)[1] are propagated in a similar manner to the surveillance satellites. The relative motion of SOs within the surveillance spacecraft field of view can be determined by considering the propagated orbit information along with attitude information. Finally, this relative motion can be used to simulate the detection capability of each spacecraft using the photometric Equations 16 through 28. All objects are assumed to have 10 cm diameter, and only the diffuse component of reflectivity is considered. These values were assumed for conservatism. Orbit propagation and detection calculations are performed for a period of 24 hours and are used to determine the number of unique object detections in that time period. By simulating the motion of known SOs from the SOC along with proven photometric relationships, the performance simulation model yields high fidelity estimations of a constellation's performance. An example of the detection capabilities of a single surveillance spacecraft over the course of a nominal day is shown in Figure 3.

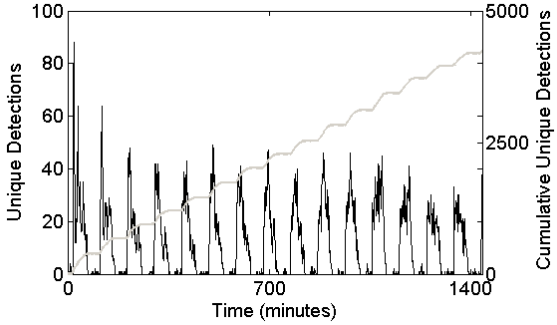

Figure 3: *Unique detections. Single Spacecraft, 500 km, 60 deg*

The simulated spacecraft undergoes 15 orbital periods in the given 24 hours sample time. Outside of the initial peak in unique detections, the number of new objects detected by the spacecraft is relatively constant through each orbital period. The relative motion of thousands of bodies is a highly nonlinear function whose performance varies over any given 24 hour period. However, a 24 hour sample period is deemed sufficient for this analysis in that the decrease in unique detections is relatively minimal over 15 orbital periods. An actual space surveillance satellite should expect to observe more objects than described here, as objects outside of the object catalog are not included.

IV.2. Objective Space

This detailed performance simulation can be utilized in an optimization algorithm to maximize the performance of a constellation of space sensors. By nature, mission design is a multidisciplinary effort, making the establishment of an objective function difficult. In many previous constellation optimization efforts, a series of multiple objective functions were establish a set of pareto-optimal solutions [26]. These algorithms develop a pareto hrontier of design points that represent tradeoffs between performance objectives. For example, many of the design tradeoffs performed in constellation

[1] www.space-track.org; accessed on 3/30/2015

optimization dealt with maximizing earth coverage while minimizing mission cost [26, 27]. These two objectives can intuitively be seen to be inversely proportional, making the definition of an optimal solution unclear. Other optimization efforts have sought to remove the pareto frontier and establish a single optimum point by requiring a minimum performance level and seeking to only minimize cost [28]. This optimization effort takes advantage of recent developments in the economics of satellite design to generate a single objective function in terms of economic return. The optimization algorithm employed here can be described as:

$$\begin{aligned} &\underset{X}{\text{maximize}} \quad f(X) = \textit{Net Present Value} \\ &\text{subject to:} \\ &\begin{bmatrix} 1 \\ 6578\,\text{km} \\ 0^\circ \end{bmatrix} \leq \begin{bmatrix} N \\ a \\ i \end{bmatrix} \leq \begin{bmatrix} 36 \\ 7678\,\text{km} \\ 100^\circ \end{bmatrix} \end{aligned} \tag{29}$$

Net Present Value (NPV) is a quantitative measure of economic return and is defined as the summation of all discounted present and future cash flows. NPV can be written as:

$$NPV = \sum(Revenue - Costs) \tag{30}$$

NPV provides a practical method for evaluating financial decisions by considering the time value of money. The design variable N is the number of satellites deployed in the constellation, a is the semi-major axis of all satellites in the constellation, and i is the inclination. There are several ways to configure the satellite constellation, yet the Walker Delta pattern [29] has been commonly used for initial constellation design, as it evenly distributes the satellites throughout the orbit environment. A Walker Delta constellation is characterized by N satellites distributed across P planes with S satellites per plane. All satellites share the same semi-major axis, eccentricity, and inclination but are phased in terms of argument of periapis and right ascension of ascending node. The ascending nodes of the P orbital planes are distributed evenly at intervals of $\frac{360}{P}$. Similarly the S satellites in each orbital plane are distributed evenly at intervals of $\frac{360}{S}$. Finally, the phase difference angle $\Delta\phi$ represents the difference in argument of periapis between adjacent planes. This phase difference angle must be an integer multiple of $\frac{360}{N}$. The Walker Delta configuration ensures that all satellites are evenly distributed throughout the orbit environment. This analysis only considers constellations of up to 36 satellites with an orbital altitude between 500 and 1300 km and inclinations ranging from equatorial to sun synchronous configurations.

The objective function utilized relies on careful calculation of economic value generated by a particular constellation as well as its lifecycle cost. The evaluation of constellation performance in terms of economic return is a valuable tool for mission planners, yet requires a detailed understanding of the true value of the space mission for its end data consumers. The prevailing market price that consumers are willing to pay for space services can be explored for various space missions, but in terms of space surveillance, Orbital Outlook, a DARPA initiative, has provided helpful metrics for quantifying the financial value of space surveillance. This initiative provides a mechanism for importing additional data from sources outside the SSN. Orbital Outlook has specified that the value of relevant SSA data is on the order of \$.01/byte [30]. This enables the calculation of revenue as follows:

$$Revenue = \frac{n_{obs} \cdot \frac{bytes}{observation} \cdot \frac{\$}{byte}}{(1+R)^T} \tag{31}$$

Where R is the required rate of return, n_{obs} is the number of observations, and T is the discount period. A three year mission lifetime is assumed with two years of development and a single year of operation. Orbital Outlook has identified specific areas of relevant data [32] to which space based sensors can contribute. These data products include the angular observations of r_A and dec relative to the spacecraft, the pixel size/location of the detected object in the field of view as well as uncertainty measurements. The total data generation capacity of a small space based sensor can be quantified at 1000 byptes per unique observation. This data product could be increased from uncorrelated track information to correlated track

information through post processing on the ground, but this added value is not considered in this analysis. After considering the revenue generated by a constellation of satellites, the lifecycle cost of deploying these satellites can be defined as follows:

$$Cost = C_{Dev} + C_{Prod} + C_{Launch} + C_{Ops} \quad (32)$$

Where C_{Dev} is the development cost, C_{Prod} is the production cost, C_{Launch} is the launch cost, and C_{Ops} is the operational cost. Development is considered as a fixed cost effort at $2,000,000 for the design, development, and testing of the satellite system. This cost is discounted at a rate R of 6% and is incurred over a two year development period. The production of a constellation of satellites is given by:

$$C_{Prod} = \frac{TFU \cdot N^{1+\frac{log(\mathcal{B})}{log(2)}}}{(1+R)^T} \quad (33)$$

This incorporates a Wright Model learning curve [31] where the incremental unit cost is reduced with increased production based on a learning curve fraction, $\mathcal{B}$. In this analysis, a protoflight development cycle is assumed with production costs incurred after one year of development.

Launch costs are assumed at $545,000 per unit based on secondary payload manifesting prices. These costs are incurred after the two year development period and are discounted at the same rate, R. Finally, operations are given as:

$$C_{Ops} = \frac{0.08 \cdot C_{Prod} + Rent \cdot t_{Ops} + 2 \cdot M}{(1+R)^T} \quad (34)$$

Where operational time is given as t_{Ops} and is modeled to scale with increasing number of satellites in addition to an overhead rate for ground station equipment. M describes the encumbered salary rate for ground station operators. It can be assumed that two ground operators are sufficient to handle the relatively small constellations considered here. The operational time for the mission is limited to one year and is discounted at rate R. The specific values for each of the parameters are given in Table 2 below.

Table 2: *Spacecraft Mass Distributions*

Parameter	Value
C_{Dev}	$2,000,000
C_{TFU}	$200,000
Learning	0.90
C_{Launch}	$545,000/unit
C_{Dev}	$3,000/month
M	$150,000
Rate	6%
Total Lifetime	3 years

V. Optimization Methodology

Performance simulation based on discrete calculations leads to an objective space that is highly discontinuous and nonlinear. Several optimization algorithms are suited for this optimization problem such as the simulated annealing and iterative mixed-integer methods, but a genetic algorithm was selected for this design problem. Many constellation optimization problems have been addressed using genetic algorithms [26] due to its stochastic nature and ability to freely explore the objective space. Genetic algorithms are meta-heuristic algorithms inspired by the reproductive and evolutionary processes found in nature. The specific genetic algorithm metrics employed in this optimization effort are shown in Table 3. A full description of these parameters can be studied further in other texts [26].

Table 3: *Summary of genetic algorithm parameters.*

Function	Value
Population Size	20
Generations	15
Elitism Count	2
Selection Method	Roulette
Crossover Fraction	75%
Mutation Fraction	1%
Constraint Evaluation	Exterior Penalty

V.1. Optimization Results

Using the optimization algorithm described here, an optimal design has been found for

a constellation consisting with $[N, a, i] = [4, 6700km, 77^\circ]$ with an overall economic return of $12.4 million by using a genetic algorithm whose performance can be measured in Figures 4 and 5. This NPV represents a return on investment of 261%.

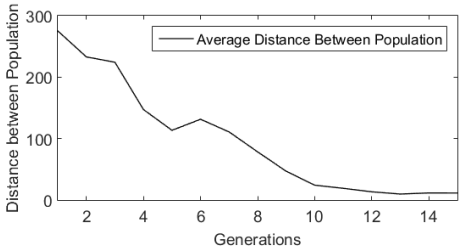

Figure 4: *Distance between design points through generations*

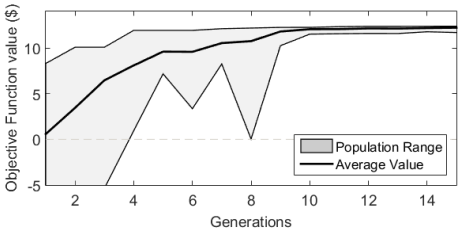

Figure 5: *Range of population objective function through generations*

Figure 4 describes the convergence of design points to a near homogeneous population at the optimal solution through consecutive generations. Figure 5 displays the range of the population's fitness in the objective space. As the population converges, the range of objective function values decreases. However, the stochastic nature of genetic algorithms ensure that the population continues to explore the sample space.

To understand the impact of each of the design variables N, a, and i, a univariate sampling of the objective space is displayed in Figures 6, 7, and 8. The effects on both economic return (NPV) as well as number of unique detections per day are analyzed. In particular, unique detections are provided as percentage of the SOC.

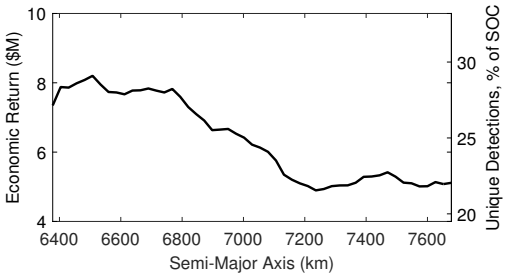

Figure 6: *Semi-Major Axis of Orbit vs Economic Return and Unique Detections*

With changing semi-major axis, it can be seen that lower altitudes are more favorable in general. The lower altitude orbits have a faster orbital period, which can in general generate more observations in a given mission time line. Given that most objects in the SO catalog are below 1200 km in altitude, any altitude below this can be expected to give a high number of observations.

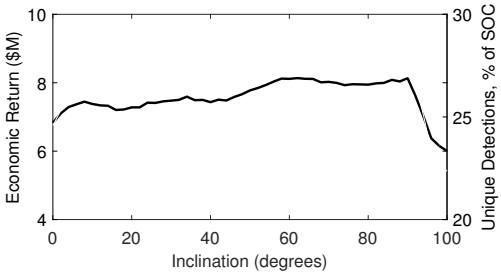

Figure 7: *Inclination of orbit vs Economic Return and Unique Detections*

By changing inclination alone, it can be seen that in general optimal orbit locations are at higher inclinations. Higher inclination orbits are typically regions that are well lit and contain largest special density of objects as many orbital planes intersect. It should be noted that for the case of a single satellite at 500 km altitude, little advantage is gained from increasing an inclination of 60 degrees to 90 degrees.

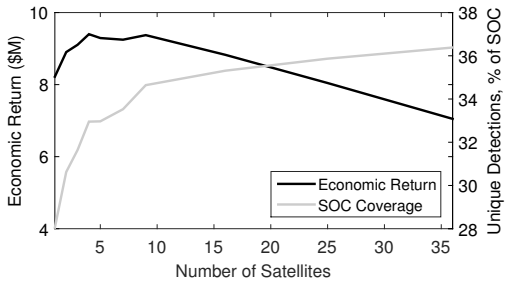

Figure 8: *Number of Satelites vs Economic Return and Unique Detections*

Finally, a uni-variate sweep of constellation size can be analyzed. By nature, increasing the number of sensors will increase the quantity of relevant data being produced by the constellation. However, there exists a point of diminishing returns, where additional satellites increase the number of unique detections at a decreasing rate. Though it can be seen that total observations are continually increasing with the number of satellites, the marginal return of these observations is less than the marginal cost of deploying additional satellites.

It should be noted that for all design points a large percentage of the current SOC is observed every day. Space Fence consistently monitors 90% of the SOC [17]. The proposed constellation stands to significantly augment current SSA efforts.

V.2. Uncertainty

Economic return calculations are heavily dependent on performance estimations as well as reliable values for financial parameters. It is prudent to quantify the uncertainty surrounding these parameters. Mission performance in terms of SO detection has been thoroughly classified through numerical modeling. Though variations in payload parameters have an effect on system performance, the values selected here are conservative. Moreover, the number of objects propagated in the simulation are far less than the actual number of space objects. The SOC simulated here does not include objects smaller than 10 cm in diameter and does not include the further increase of objects through the course of the simulation. As this optimization effort seeks to quantify the economic returns generated by mission performance, the financial parameters provided in these calculations are just as important in the objective function value as detection performance. As the coefficient of economic value per relevant byte of data is a driving factor for the overall objective function, a sensitivity analysis of varying payment rates was considered. At several values of $/byte payment rate a complete optimization algorithm was performed. The results shown in Figure 9 capture the sensitivity of the optimization effort with respect to the changes in the price of data generated by the constellation.

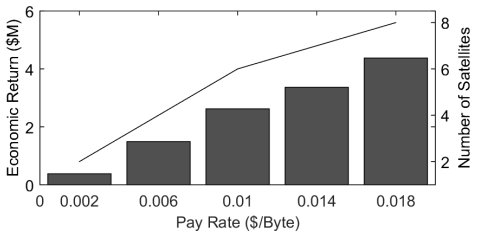

Figure 9: *Sensitivity of Economic Return and Constellation size to Payment Rate*

It is evident that the level of economic return is highly dependent on payment rate. However, the designs shown here generate a positive economic return at a payment rate 80% less than the expected value. The significant performance-to-cost capability of small satellite constellations enables sufficient contingency against changes in payment rate. For each optimal point generated generated across varying payment rates, semi-major axis and inclination remained constant at 6700 km and 70°respectively. However, as the payment rate increases, the optimal number of satellites increases as well. The higher payment rate raises the point of diminishing returns displayed in Figure 8.

VI. Conclusion

The design process proposed here includes the design of a spacecraft payload, an analysis of the detection constraints, and an optimization effort to maximize constellation performance. The prospect of deploying a constellation of small satellites for space situational awareness

is promising in terms of economic return and overall detection capability. The total returns produced by the optimal configuration amount to over 2.5 times the required costs while observing nearly 40% of the SOC each day. The performance simulation and quantification of economic return provide compelling reasons to pursue the development of such a constellation. Quantifying the financial value of mission performance enables mission planners to truly evaluate the economics of a space mission. Optimization based on economic return provides a powerful tool for aerospace firms and can give confidence to pursue new endeavors.

References

[1] Kessler, Donald J., Johnson, Nicholas L., J.C. Liou, and Mark Matney. "The Kessler Syndrome: Implications to Future Space Operations" pp 47-61. February 6, 2010. *Paper AAS 10-016, Advances in the Astronautical Sciences*.

[2] NASA, "Handbook for Limiting Orbital Debris," 2008.

[3] Joint Space Operations Command *US Air Force Fact Sheet: Joint Functional Component Command for Space* December 2012: Vandenberg Air Force Base.

[4] Committee on Space Debris, "Orbital Debris: A Technical Assessment," 1995.

[5] J. C. Liou, editor, "Update on Three Major Debris Clouds," *Orbital Debris Quarterly News*, 14(2), April 2010, www.orbitaldebris.jsc.nasa.gov.

[6] "NASA Orbital Debris FAQ," March 2012, available via http://orbitaldebris.jsc.nasa. gov/faqs.html

[7] S. Kan, China's Anti-Satellite Weapon Test, CRS Report for Congress, Congressional Research Service, The Library of Congress (April 2007).

[8] T. S. Kelso, Analysis of the Iridium 33-Cosmos 2251 Collision, in: *Advanced Maui Optical and Space Surveillance Technologies Conference*, 2009.

[9] Murray, Craig. "China's Missile Launch May Have Tested Part of a New AntiSatellite Capability" *U.S.-China Economic and Security Review Commission* May 22, 2013.

[10] Christiansen, Eric L. "Meteoroid/Debris Shielding," NASA Johnson Space Center, *TPâĹŠ2003-210788*, August 2003.

[11] D.S. McKnight and F.R.D. Pentino, "New Insights on the Orbital Debris Collision Hazard at GEO," *Acta Astronautica*, Vol. 85, No. 0, 2013, pp. 73-82, http://dx.doi.org/10/1016/j/actaastro.20 12.12.006.

[12] "National Space Policy of the United States of America," June 28, 2010, available via http://www.whitehouse.gov

[13] Scaparrotti, Curtis M. "Joint Publication 3-14 Space Operations" May 29, 2013: *US Army Joint Chiefs of Staff*.

[14] US Air Force Chief Scientist "Joint Functional Component Command for Space" pp 120-138. May 15, 2010. *US Air Force* AF/ST-TR-10-01-PR.

[15] Butler, Amy. "Space Situational Awareness Key to AF's 2014 Plan" *Military.com* April 16, 2013, available via http://www.military.com/daily-news/2013/04/16/space-situational-awareness-key-to-afs-2014-plan.html

[16] United Nations Committee on the Peaceful Uses of Outer Space, "Report of the Scientific and Technical Subcommittee on its forty-seventh session, held in Vienna from 8 to 19 February 2010," AC.105/958, 11 March 2010.

[17] "Lockheed Martin Selected to Provide U.S. Air Force with Space Fence Radar to Safeguard Space Resources" Lockheed Martin Press Release, June 3, 2014, available via http://www.lockheedmartin.com/us/news/press-releases/2014/june/140603-mst-lm-selected-to-provide-us-air-force-with-space-fence-radar.html

[18] "Space Based Space Surveillance" *Air Force Space Command*. February 25, 2015, available via http://www.afspc.af.mil/library/factsheets/factsheet.asp?id=20523

[19] R. Sridharan and Antonio F. Pensa, "U.S. Space Surveillance Network Capabilities," in *Characteristics and Consequences of Space Debris and Near-Earth Objects*, Proc. SPIE 3434, 88-100, (1998).

[20] Kolomenkin, M., Polak, S., Shimshoni, I., and Lindenbaum, M., "A Geometric Voting Algorithm for Star Trackers," Haifa University, Haifa, Israel.

[21] Coder, R., and Holzinger, M., "Multi-Objective Design of Optical Systems for Space Situational Awareness," Guggenheim School of Aerospace Engineering, Georgia Institute of Technology, Atlanta, GA, Feb. 2015.

[22] Schildknecht, T., âĂIJOptical Astrometry of Fast Moving Objects Using CCD Detectors,âĂİ Institut fur Geodasie und Photogrammetrie, Zurich, Switzerland, 1994.

[23] Schildknecht, T., Hugentobler, U., and Verdun, A., âĂIJAlgorithms for Ground Based Optical Detection of Space Debris,âĂİ, Astronomical Institute, University of Bern, Switzerland, 1995.

[24] Worthy, Johnny L., Holzinger, Marcus J., and Fujimoto, Kohei, "Optical Sensor Constraints on Space Object Detection and Admissible Regions," *AAS 13-707* Hilton Head, SC, 2013.

[25] M. Mulrooney, M. J. Matney, M. D. Hejduk, and E. S. Barker, "An Investigation of Global Albedo Values," *Proceedings of the Advanced Maui Optical and Space Surveillance Technologies Conference*, 2008.

[26] Ely, T.A., Crossley, W.A., and Williams, E.A. "Satellite Constellation Design for Zonal Coverage Using Genetic Algorithms," *The Journal of the Astronautical Sciences*, Vol. 47, Nos. 3 and 4, July-Dec. 1999, pp. 207-228

[27] Long, F., *Satellite Network Robust QoS-aware Routing*. Beijing: National Defense Industry Press, 2014

[28] Irene, I.A., Olds, J.R. "Design and Deployment of a Satellite Constellation Using Collaborative Optimization," *Journal of Spacecraft and Rockets*, Vol. 41, No. 6, Nov.-Dec. 2004, pp. 956-963

[29] Walker, J. G., "Some Circular Patterns Providing Continuous Whole Earth Coverage," *Journal of the British Interplanetary Society*, Vol. 24, No. 7, 1971, pp. 369-384.

[30] Blake, T., Sanchez, M., and Bolden, M., "Orbital Outlook: Data-centric Competition Based Space Domain Awareness (SDA)," *Defense Advanced Research Projects Agency, CENTRA Technology*, Distribution Statement "A"

[31] Wertz, J.R., Larson, W.J. *Space Mission Analysis and Design, Third Edition*, Hawthorne: Microcosm Press, Springer, 1999

[32] Koblick, D.,Goldsmith, A., Klub, M., Mangus, P., "Ground Optical Signal Processing Architecture for Contributing Space-Based SSA Sensor Data," *Millenium Space Systems, Air Force Research Labratory, Raytheon, Schafer Corporation, CENTRA Technology, Defense Advanced Research Projects Agency*, Distribution Statement "A"